Electronic Circuit in the Two-Scroll Hyperchaotic System with a Unique Saddle-Point Rest Point and its Synchronization via Integral Sliding Mode Control

Mujiarto, Ahmad Faisal Mohamad Ayob, Sundarapandian Vaidyanathan, Aceng Sambas, Khaled Benkouider
Mohd Kamal Mohd Nawawi, Kamal Khalid, and Elissa Nadia Madi

***Abstract*—A new 4-D two-scroll hyperchaotic system with three quadratic nonlinearities is detailed in this research paper. It is shown that the new hyperchaotic system has a unique saddle-point rest point at the origin and it exhibits self-excited attractor. A detailed stability analysis is carried out for the new hyperchaotic system.It is also proved that the new hyperchaotic system has multistability with coexisting attractors. Next, we invoke integral sliding mode control for the global self-synchronization of the new hyperchaotic system taken as leader-follower systems.An electronic circuit design of the new two-scroll hyperchaotic system is developed in MultiSim, which is beneficial for engineering applications.**

***Index Terms*—Hyperchaos; hyperchaotic systems; rest points; multi-stability; sliding mode control; circuit simulation.**

I. INTRODUCTION

HYPERCHAOTIC systems are defined as chaotic systems having two or more positive Lyapunov exponents [1]. Hyperchaotic systems exhibit more complexity than the chaotic systems and hence they have important engineering applications such as neural networks [2], chemical reactors [3], mechanical systems [4], wind turbine [5]-[6], robotics [7], electronic circuit [8]-[10], finance systems [11][12], etc.

In this research work, a new 4-D two-scroll hyperchaotic system with three quadratic nonlinearities is proposed and the properties of the new hyperchaotic system are analyzed in detail.It is established that the new two-scroll hyperchaotic system has a unique saddle-point rest point at the origin. Hence, it follows that the new hyperchaotic system has hidden attractor [13]-[15].

Multistablity is a special property of chaotic and hyperchaotic systems which is the coexistence of attractors for same parameter set but different initial conditions [16]-[19]. In this work,it is also established that the new two-scroll hyperchaotic system has multistability with coexisting attractors.

Control and synchronization of chaotic and hyperchaotic systems are important research topics in the chaos literature [20]-[25]. Many control methods are used in control engineering for chaotic systems such as nonlinear control [20], adaptive control [21], backstepping control [22], sliding mode control [23]-[24], fuzzy logic control [25], etc. In this research work, we use integral sliding mode control for the global self-synchronization of the new hyperchaotic system. Sliding mode control has attractive properties such as finite-time convergence, robust to parameter variations, etc [26].

Section 2 describes the modelling of the new two-scroll hyperchaotic system with three quadratic nonlinear terms. Section 3 provides a dynamic analysis of the new two-scroll hyperchaotic system. Section 4 deals with the global self-synchronization of the new two-scroll hyperchaotic system considered as leader-follower systems using integral sliding mode control. Section 5 contains the circuit simulation of the new two-scroll hyperchaotic system using MultiSim.

II. A NEW TWO-SCROLL HYPERCHAOTIC SYSTEM

In this work, we consider a new 4-D system with three quadratic nonlinear terms:

$$\begin{cases} \dot{y}_1 = a(y_2 - y_1) + py_2y_3 - y_4 \\ \dot{y}_2 = by_1 - dy_1y_3 - y_4 \\ \dot{y}_3 = y_1y_2 - cy_3 \\ \dot{y}_4 = dy_2 \end{cases} \tag{1}$$

In (1), $Y = (y_1, y_2, y_3, y_4)$ is the state and a, b, c, d, p are positive constants. We show that the system (1) exhibits a

Manuscript received June 3, 2023; revised November 29, 2023. This project is funded by the Universiti Utara Malaysia and Universitas Muhamadiyah Tasikmalaya.

Mujiarto is an Associate Professor in the Department of Mechanical Engineering, Universitas Muhammadiyah Tasikmalaya, Indonesia and Postdoctoral Research in the Department of Mechanical Engineering, Universiti Malaysia Terengganu, Malaysia (email: mujiarto@umtas.ac.id)

Ahmad Faisal Mohamad Ayob is an Associate Professor in the Faculty of Ocean Engineering Technology and Informatics, Universiti Malaysia Terengganu, Terengganu, Malaysia (email: ahmad.faisal@umt.edu.my).

Sundarapandian Vaidyanathan is a Professor in the Research and Development Centre, Vel Tech University, Avadi, Chennai-600062, Tamil Nadu, India (email: sundar@veltech.edu.in).

Aceng Sambas is an Assistant Professor in the Faculty of Informatics and Computing, Universiti Sultan Zainal Abidin, Gong Badak, Kuala Terengganu, Malaysia and an Assistant Professor in the Department of Mechanical Engineering, Universitas Muhammadiyah Tasikmalaya, Indonesia (email: acengsambas@unisza.edu.my).

Khaled Benkouider is an Associate Professor in Department of Electronics, Faculty of technology, Badji-Mokhtar University, Annaba-23000, Algeria (email: khaled.benkouider@univ-annaba.dz).

Mohd Kamal Mohd Nawawi is an Associate Professor in the Institute of Strategic Industrial Decision Modeling, School of Quantitative Sciences, Universiti Utara Malaysia, 06010, UUM Sintok, Kedah, Malaysia (Corresponding email: mdkamal@uum.edu.my).

Kamal Khalid is an Associate Professor in the Institute of Strategic Industrial Decision Modeling, School of Quantitative Sciences, Universiti Utara Malaysia, 06010, UUM Sintok, Kedah, Malaysia (email: kamal@uum.edu.my).

Elissa Nadia Madi is an Assistant Professor in the Faculty of Informatics and Computing, Universiti Sultan Zainal Abidin, Gong Badak, Kuala Terengganu, Malaysia (email: elissa@unisza.edu.my).

hyperchaotic attractor when the parameters are taken as

$$a = 8,\ b = 32,\ c = 3,\ d = 3,\ p = 0.2 \tag{2}$$

For MATLAB simulations, we take the initial values of the 4-D system (1) as

$$y_1(0) = 0.2,\ y_2(0) = 0.3,\ y_3(0) = 0.3,\ y_4(0) = 0.2 \tag{3}$$

Using Wolf algorithm [27], we calculate the Lyapunov characteristic exponents (LCE) for the system (1) for the parameter values (2) and the initial state (3) for $T = 1E5$ seconds as follows:

$$\mu_1 = 0.7223,\ \mu_2 = 0.2449,\ \mu_3 = 0,\ \mu_4 = -11.9546 \tag{4}$$

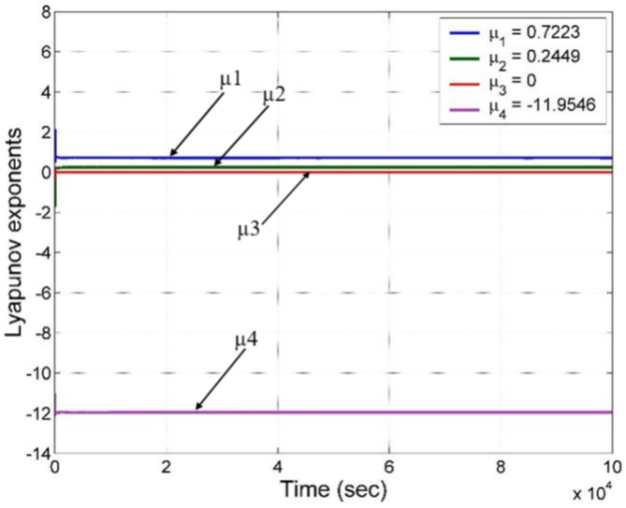

Fig. 1: Lyapunov exponents of the new 4-D system (1) for (a, b, c, d, p)=(8,32,3,3,0.2)

Fig. 1 shows the Lyapunov exponents of the new hyperchaotic system (1) for the parameter values (a, b, c, d, p)=(8,32,3,3,0.2).

The system (1) is hyperchaotic since it possesses two positive Lyapunov characteristic exponents μ_1 and μ_2. As the sum of the LCE values in (4) is negative, the system (1) is also dissipative.

Fig. 2 shows the MATLAB plots of the new hyperchaotic system (1) in various coordinate planes for (a, b, c, d, p)=(8,32,3,3,0.2) and $Y(0)$=(0.2,0.3,0.3,0.2).

From Fig. 2, it is clear that the hyperchaotic system (1) is equipped with a two-scroll hyperchaotic attractor.

III. DYNAMIC ANALYSIS OF THE NEW TWO-SCROLL HYPERCHAOTIC SYSTEM

A. Rest Points of the New Hyperchaotic System

The rest points of the new two-scroll hyperchaotic system are calculated by means of finding the roots of the following algebraic system of equations:

$$a(y_2 - y_1) + py_2y_3 - y_4 = 0 \tag{5a}$$

$$by_1 - dy_1y_3 - y_4 = 0 \tag{5b}$$

$$y_1y_2 - cy_3 = 0 \tag{5c}$$

$$dy_2 = 0 \tag{5d}$$

Solving (5d), we get $y_2 = 0$.

Substituting $y_2 = 0$ in (5c), we get $y_3 = 0$.

Next, we put $y_2 = y_3 = 0$ into equations (5a) and (5b) and obtain the following:

$$ay_1 + y_4 = 0 \tag{6a}$$

$$by_1 - y_4 = 0 \tag{6b}$$

Adding (6a) and (6b), we get $(a + b)y_1 = 0$.

Since $a > 0$ and $b > 0$, it follows that $y_1 = 0$.

Substituting $y_1 = 0$ into (6a), we get $y_4 = 0$. Hence, $K_0 = (0, 0, 0, 0)$ is the unique rest point of the two-scroll hyperchaotic system (1).

To investigate the stability of K_0, we determine the Jacobian matrix of the two-hyperchaotic system (1) at the rest point K_0 for the hyperchaotic case (a, b, c, d, p) =(8,32,3,3,0.2) as follows:

$$J_0 = \begin{bmatrix} -8 & 8 & 0 & -1 \\ 32 & 0 & 0 & -1 \\ 0 & 0 & -3 & 0 \\ 0 & 3 & 0 & 0 \end{bmatrix} \tag{7}$$

The spectral values of the Jacobian matrix J_0 are numerically estimated in MATLAB as follows:

$$\alpha_1 = -3,\ \alpha_2 = -20.5780,\ \alpha_3 = 0.4821,\ \alpha_4 = 12,0959 \tag{8}$$

This pinpoints that K_0 is a saddle-point and unstable rest point for the two-scroll hyperchaotic system (1). Hence, we deduce that the system (1) has a self-excited two-scroll hyperchaotic attractor.

B. Bifurcation and Lyapunov Exponents

In this section, we delve into the dynamic characteristics of the proposed four-dimensional hyperchaotic system (1), examining how these dynamics evolve in relation to various parameters. Our exploration involves the utilization of tools such as the Lyapunov exponents spectrum, bifurcation diagram, and phase plots to gain a comprehensive understanding of the system's behavior and the intricate interplay with its associated parameters.

1) Fix b = 32, c = 3, d = 3, p = 0.2, and vary a: In the context of a fixed parameter set where *b* = 32, *c* = 3, *d* = 3, and *p* = 0.2, and the control parameter a is systematically adjusted within the range [0.5, 8], the bifurcation diagram and Lyapunov exponents spectrum are presented in Fig. 3 and Fig. 4 , respectively.

For values of a in the interval [0.5, 1.2], System (1) exhibits a periodic nature, characterized by one zero and three negative Lyapunov exponents, as depicted in Fig. 5(a). Specifically, at a=0.5, the corresponding Lyapunov exponents are detailed as follows: LE1 = 0, LE2 = -0.407, LE3 = -1.249, and LE4 = -1.852.

Upon entering the range $a \in [1.2, 6]$, System (1) undergoes a transition to chaotic behavior, with a single positive Lyapunov exponent, showcased in Fig. 5(b). Notably, at *a* = 3, the specific Lyapunov exponents are outlined as follows: LE1 = 0.632, LE2 = 0, LE3 = -0.836 and LE4 = -5.795. The associated Kaplan-Yorke dimension maintains a fractional value of 2.756 during this chaotic regime.

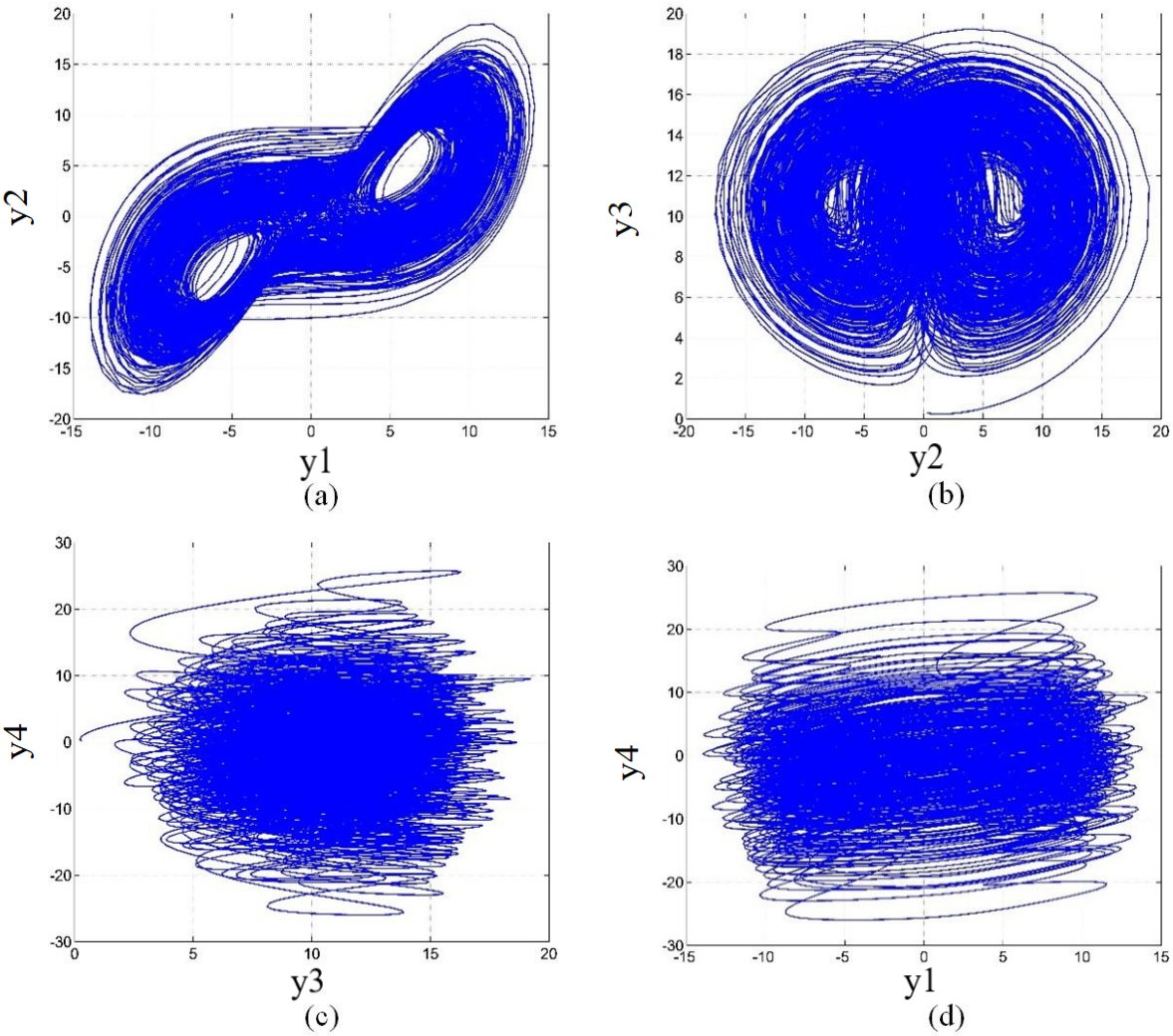

Fig. 2: MATLAB 2-D plots of the new 4-D two-scroll hyperchaotic system (1) for (a, b, c, d, p)=(8,32,3,3,0.2) and $Y(0)$=(0.2,0.3,0.3,0.2).

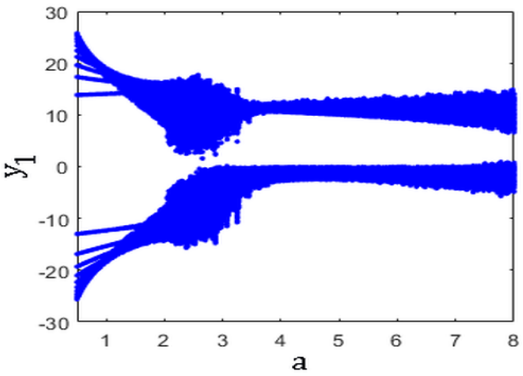

Fig. 3: Bifurcation Diagram for varying paramater *a*

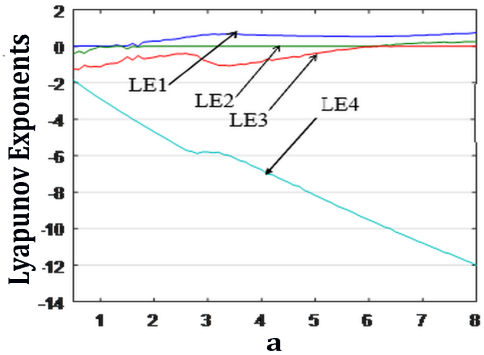

Fig. 4: Lyapunov exponents for varying paramater *a*

Extending further into the range $a \in [6, 8]$, System (1) reveals hyperchaotic behavior, marked by the presence of two positive Lyapunov exponents, as illustrated in Fig. 5(c). Specifically, at $a = 7$, the corresponding Lyapunov exponents are noted as follows: LE1 = 0.589, LE2 = 0.197, LE3 = 0, and LE4 = -10.787. The Kaplan-Yorke dimension maintains a fractional value of 3.073 during this chaotic regime.

This detailed examination provides a coherent narrative of the dynamic transformations experienced by System (1) across varying values of the control parameter *a*, shedding light on its periodic, chaotic, and hyperchaotic behaviors.

2) Fix a = 8, c = 3, d = 3, p = 0.2, and vary b: When the parameters *a*, *c*, and *d* are held constant at specific values ($a = 8$, $c = 3$, $d = 3$, and $p = 0.2$), the control

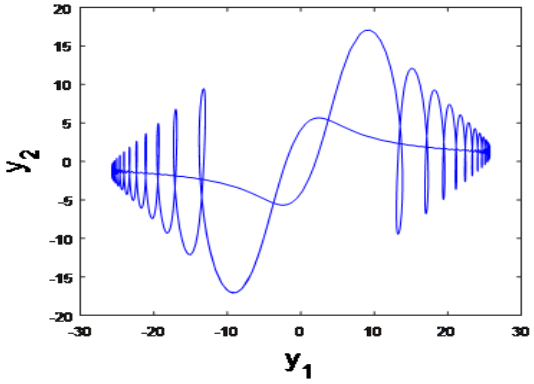

(a)

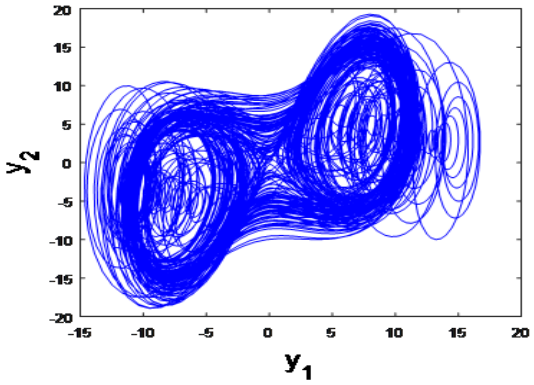

(b)

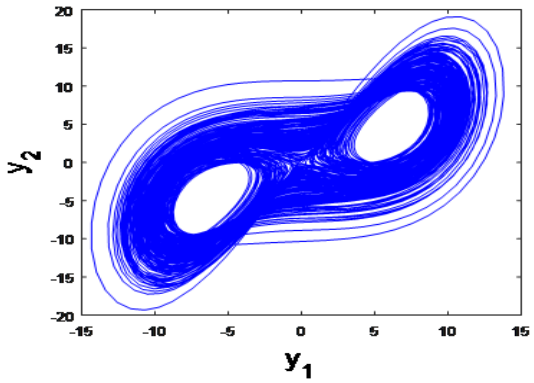

(c)

Fig. 5: Phase plots of system (1) for specifics values of the control parameter a: (a). a = 0.5, (b). a = 3 and (c). a = 7

parameter b undergoes variation within the range [0, 32]. The resulting Lyapunov exponents spectrum and bifurcation diagram for the new system are illustrated in Fig. 6 and Fig. 7, respectively.

Within the range $b \in [0, 9]$, System (1) displays periodic behavior, characterized by one zero and three negative Lyapunov exponents, as demonstrated in Fig. 8(a). For instance, at b = 2, the corresponding Lyapunov exponents are detailed as follows: LE1 = 0, LE2 = -0.260, LE3 = -1.754, and LE4 = -8.985.

Transitioning into the interval $b \in [9, 12]$, System (1) undergoes a shift towards chaotic behavior, featuring one positive Lyapunov exponent, as depicted in Fig. 8(b). Specifically, at b = 11, the specific Lyapunov exponents are outlined as follows: LE1 = 0.191, LE2 = 0, LE3 = -0.109, and LE4 = -11.082. Notably, the Kaplan-Yorke dimension maintains a fractional value of 3.007 during this chaotic phase.

As b continues into the range [12, 32], the system further evolves into a state of hyperchaos, characterized by two positive Lyapunov exponents, as shown in Fig. 8(b)(c). For instance, at b = 20, the corresponding Lyapunov exponents are LE1 = 0.415, LE2 = 0.356, LE3 = 0, and LE4 = -11.773. Importantly, the Kaplan-Yorke dimension assumes a fractional value of 3.066 during this intriguing hyperchaotic phase.

This comprehensive analysis offers a cohesive account of the dynamic changes observed in System (1) as the control parameter "b" varies. It provides insights into the system's periodic, chaotic, and hyperchaotic behaviors, offering a clearer understanding of its intricate dynamics across different values of the control parameter.

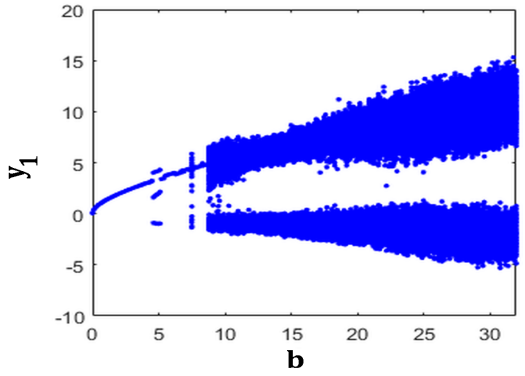

Fig. 6: Bifurcation Diagram for varying paramater b

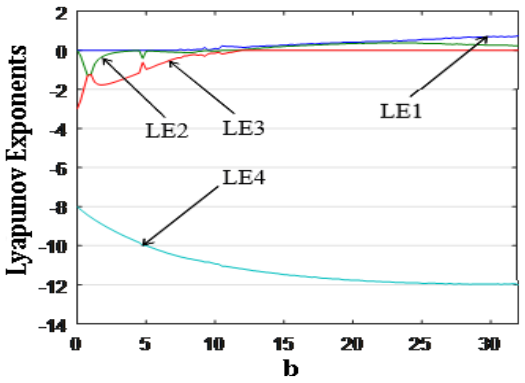

Fig. 7: Lyapunov exponents for varying paramater b

3) Fix a = 8, b = 32, d = 3, p = 0.2 and vary c: When the values of parameters a, b, and d are kept constant at specific settings (a = 8, b = 32, d = 3, and p = 0.2), the control parameter c experiences variation within the interval [0, 3]. Fig. 9 and Fig. 10 visually represent the Lyapunov exponents spectrum and bifurcation diagram for the new system.

In the segments where c lies within ([0, 0.2], [1.5, 2.3]), System (1) demonstrates periodic behavior, featuring one zero and three negative Lyapunov exponents, as showcased in Fig. 11(a). For example, at c = 1.7, the corresponding Lyapunov exponents are LE1 = 0, LE2 = -1.531, LE3 = -4.028, and LE4 = -4.146.

Moving into the range $c \in [2.3, 2.4]$, System (1) undergoes a transition towards chaotic dynamics, characterized by the

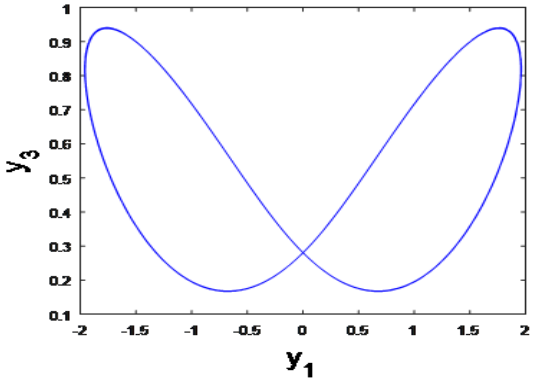

(a)

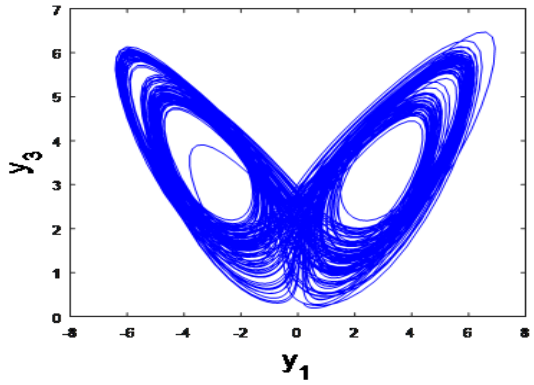

(b)

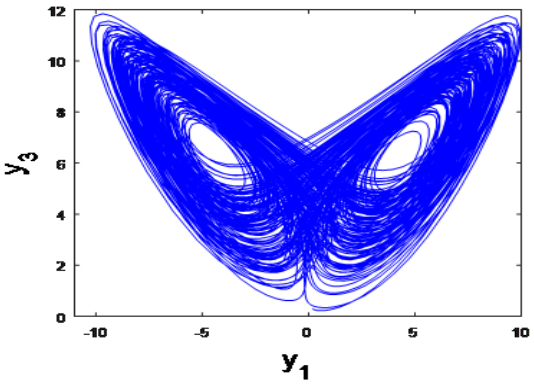

(c)

Fig. 8: Phase plots of system (1) for specifics values of the control parameter b: (a). b = 2, (b). b = 11 and (c). b = 20

emergence of one positive Lyapunov exponent, as illustrated in Fig. 11(b). Specifically, at c = 2.34, the specific Lyapunov exponents are detailed as follows: LE1 = 0.015, LE2 = 0, LE3 = -0.004, and LE4 = -10.348. Notably, the Kaplan-Yorke dimension maintains a fractional value of 3.001 during this chaotic phase.

In the intervals ([0.2, 1.5], [2.4, 3]), the system evolves further into a state of hyperchaos, marked by two positive Lyapunov exponents, as depicted in Fig. 11(c). For instance, at c = 1, the corresponding Lyapunov exponents are LE1 = 0.663, LE2 = 0.285, LE3 = -5.496, and LE4 = -5.509. Significantly, the Kaplan-Yorke dimension assumes a fractional value of 3.095 during this intriguing hyperchaotic phase.

This in-depth analysis provides a coherent depiction of the dynamic transformations observed in System (1) as the control parameter "c" undergoes variation. It yields insights into the system's periodic, chaotic, and hyperchaotic behaviors, enhancing our understanding of its complex dynamics across different values of the control parameter.

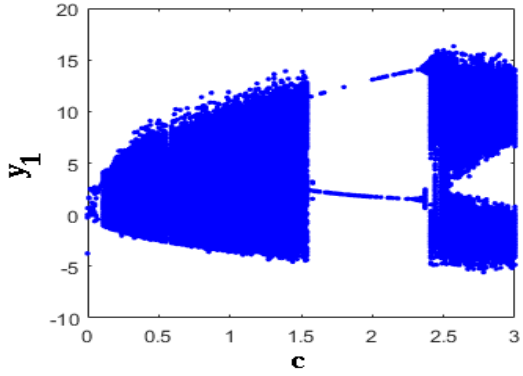

Fig. 9: Bifurcation Diagram for varying paramater c

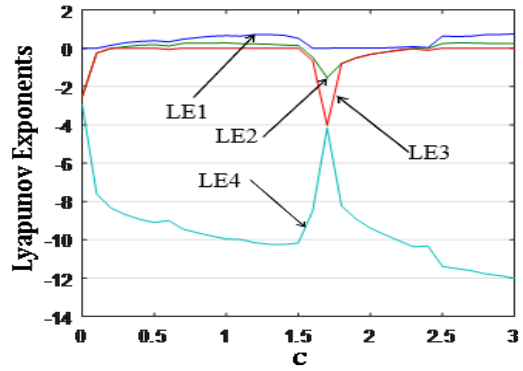

Fig. 10: Lyapunov exponents for varying paramater c

4) Fix a = 8, b = 32, c = 3, p = 0.2 and vary d: In the scenario where parameters a, b, c, and p are held constant at specific values (a = 8, b = 32, c = 3, and p = 0.2), the control parameter d is subjected to variation within the range [0.1, 3]. The Lyapunov exponents spectrum and bifurcation diagram for the novel system are visually represented in 12 and Fig. 13, respectively.

Within the interval where $d \in$ [0.1, 0.15], System (1) exhibits periodic behavior with two zero Lyapunov exponents, as illustrated in Fig. 14(a). For instance, at d=0.11, the corresponding Lyapunov exponents are detailed as follows: LE1 = 0, LE2 = -0.003, LE3 = -5.496, and LE4 = -5.509.

Continuing within the interval [0.15, 0.70], the system undergoes a transition into chaotic behavior, maintaining one positive Lyapunov exponent, as showcased in Fig. 14(b). For example, at d = 0.3, the specific Lyapunov exponents are outlined as follows: LE1 = 0.503, LE2 = 0, LE3 = -0.319 and LE4 = -11.186. Notably, the Kaplan-Yorke dimension maintains a fractional value of 2.060, and the overall Kaplan-Yorke dimension is 3.016.

As the parameter d extends into the range [0.7, 3], System (1) reveals a hyperchaotic state with two positive Lyapunov exponents, as depicted in Fig. 14(c). At d = 2.5, the corresponding Lyapunov exponents are LE1 = 0.736, LE2 = 0.192, LE3 = 0, and LE3 = -11932. Additionally, the Kaplan-Yorke dimension assumes a value of 3.078 during this hyperchaotic phase.

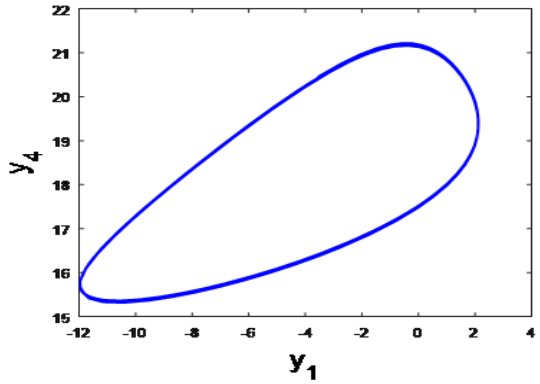

(a)

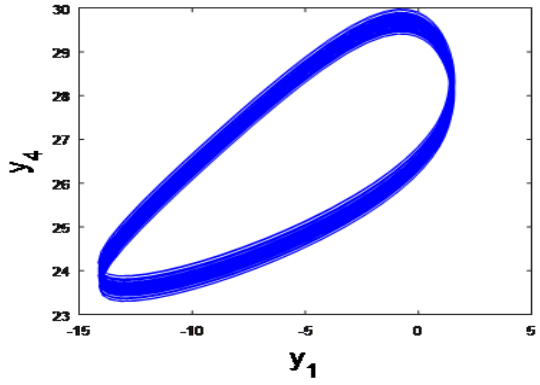

(b)

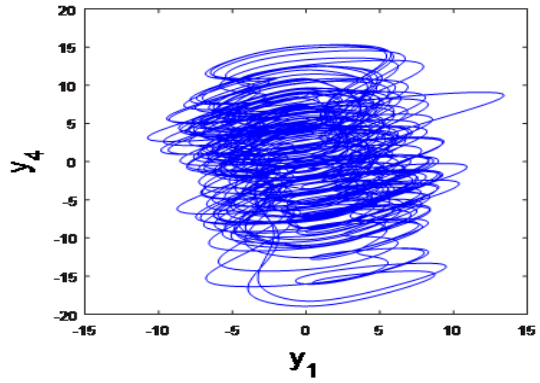

(c)

Fig. 11: Phase plots of system (1) for specifics values of the control parameter c: (a). c = 1.7, (b). c = 2.34 and (c). c = 1

This thorough examination offers a clear representation of the dynamic changes in System (1) as the control parameter "d" is altered. It provides valuable insights into the system's periodic, chaotic, and hyperchaotic behaviors, contributing to an enhanced comprehension of its intricate dynamics across varying values of the control parameter.

5) Fix a = 8, b = 32, c = 3, d = 3 and vary p: Here, the parameters a, b, c, and d are fixed at particular values (a = 8, b = 32, c = 3, and d = 3), while, the control parameter p undergoes variation within the interval [-1, 1]. The Lyapunov exponents spectrum and bifurcation diagram for the novel system are graphically depicted in Fig. 15 and Fig. 16, respectively.

In the range where $p \in$ [-1, -0.4], System (1) displays periodic behavior, as depicted in Fig. 17(a). Specifically, at p = -0.6, the associated Lyapunov exponents are detailed as

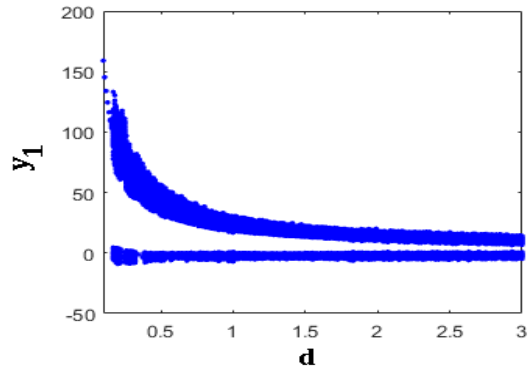

Fig. 12: Bifurcation Diagram for varying paramater d

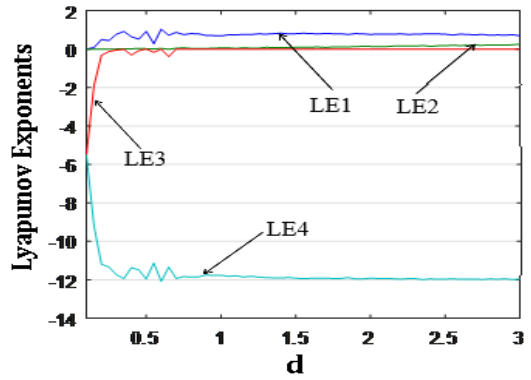

Fig. 13: Lyapunov exponents for varying paramater d

follows: LE1 = 0, LE2 = -2.164, LE3 = -2.167, and LE4 = -6.670.

Advancing within the interval [-0.4, -0.3], the system undergoes a shift towards chaotic dynamics, maintaining one positive Lyapunov exponent, as illustrated in Fig. 17(b). For instance, at p = -0.35, the specific Lyapunov exponents are outlined as follows: LE1 = 0.268, LE2 = 0, LE3 = -0.412, and LE4 = -10.856. Notably, the Kaplan-Yorke dimension retains a fractional value of 2.651.

As the parameter "p" varies within the interval [-0.3, 1], System (1) exhibits a hyperchaotic state characterized by two positive Lyapunov exponents, as illustrated in Fig. 17(c). When p is set to 4, the corresponding Lyapunov exponents are LE1 = 0.732, LE2 = 0.168, LE3 = 0, and LE4 = -11.901. Additionally, the Kaplan-Yorke dimension attains a value of 3.076 during this hyperchaotic phase.

This in-depth analysis provides a vivid depiction of the dynamic transformations in System (1) with changes in the control parameter "p."

C. Multistability of the New 4D Hyperchaotic System

The hyperchaotic system (1) demonstrates the existence of various attractors even when the parameters remain constant. Take into account two separate starting points for the new 4D hyperchaotic system (1): X_{01} = (3, 3, 3, 3) and X_{02} = (3, 0, 0, 3). The state trajectory linked to X_{01} is depicted in blue, while the state trajectory associated with X_{02} is illustrated in red.

Set the parameters to a = 8, b = 8.7, c = 3, d = 0, and p = 0.2. In this configuration, the new 4D Hyperchaotic

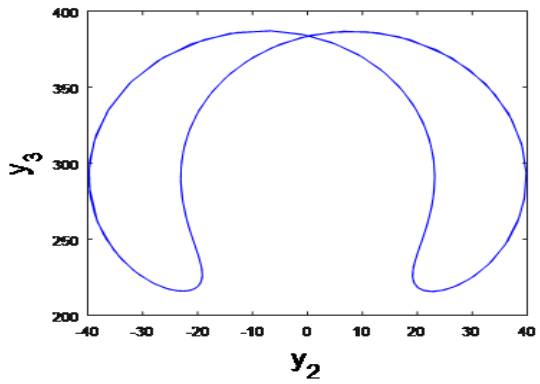

(a)

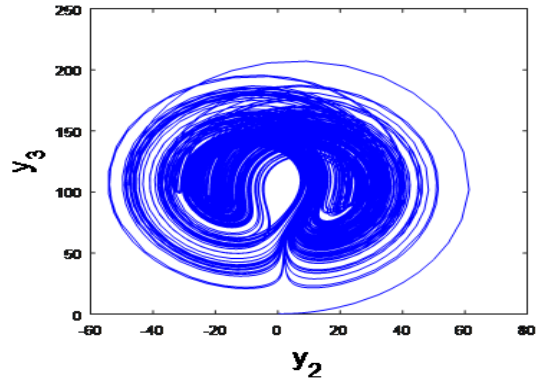

(b)

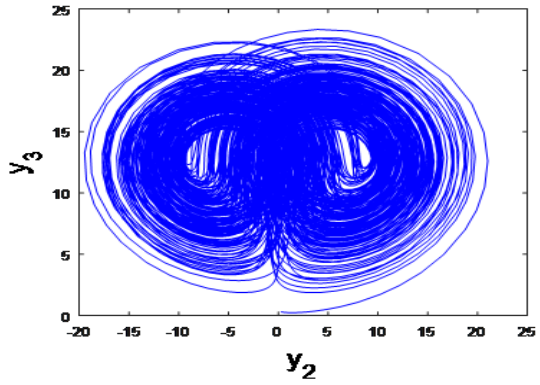

(c)

Fig. 14: Phase plots of system (1) for specifics values of the control parameter d: (a). d = 0.11, (b). d = 0.3 and (c). d = 2.5

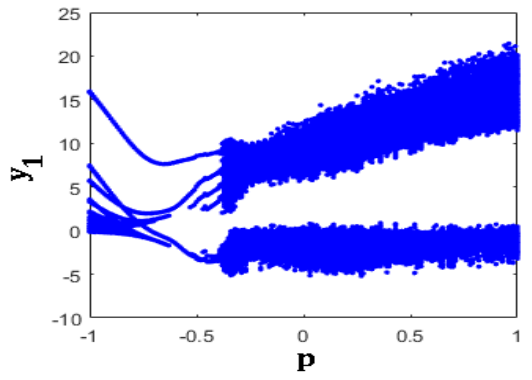

Fig. 15: Bifurcation Diagram for varying paramater p

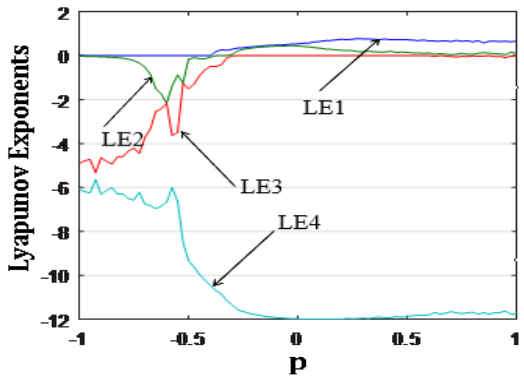

Fig. 16: Lyapunov exponents for varying paramater p

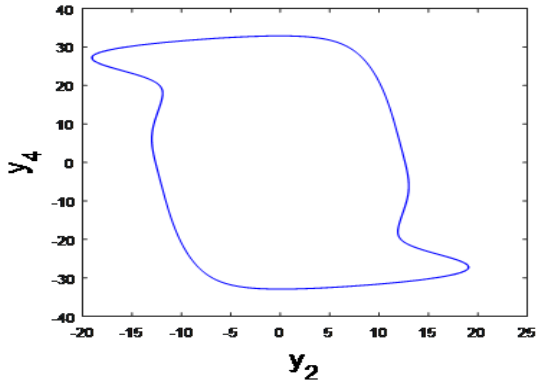

(a)

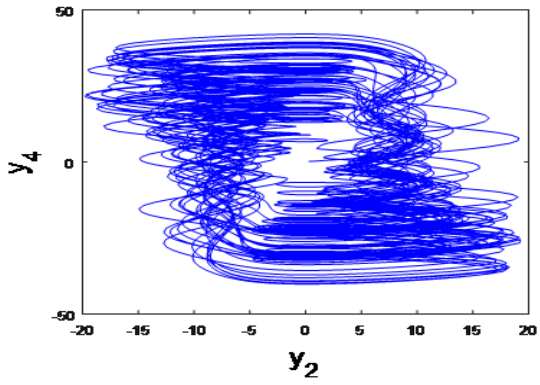

(b)

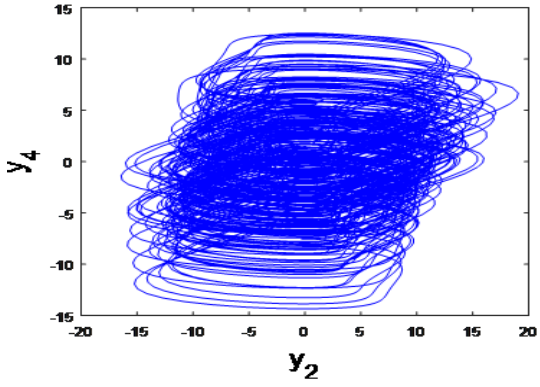

(c)

Fig. 17: Phase plots of system (1) for specifics values of the control parameter p: (a). p = -0.6, (b). p = -0.35 and (c). p = 0.4

System (1) converges to two distinct coexisting periodic orbits based on its initial conditions, as depicted in Fig. 18(a). Adjust the parameters to a = 8, b = 9.1, c = 3, d = 3, and p = 0.2. Under these settings, the new 4D Hyperchaotic System (1) exhibits two varied behaviors depending on its starting points, as illustrated in Fig. 18(b). When initiated from X_{01}, the system generates a chaotic attractor, whereas it demonstrates periodic behavior when initiated from X_{02}. Maintain the parameters at a = 8, b = 9.5, c = 3, d = 3, and p = 0.2. The 4D system (1) showcases two different behaviors based on its starting conditions, as shown in Fig. 18(c). Initiating from X_{01} results in periodic behavior, while starting from X_{02} leads to the generation of a chaotic attractor. Set the parameters to a = 8, b = 22, c = 3, d = 3, and p = 0.2. Under these conditions, the 4D system (1) displays the coexistence of two distinct hyperchaotic attractors, as depicted in Fig. 18(d).

IV. GLOBAL SYNCHRONIZATION VIA ISMC

As a control application, we invoke integral sliding mode control (ISMC) for the global synchronization between the states of the new two-scroll hyperchaotic systems taken as *leader-follower* systems.

As the leader system, we take the two-scroll hyperchaotic system

$$\begin{cases} \dot{y}_1 &= a(y_2 - y_1)_p y_2 y_3 - y_4 \\ \dot{y}_2 &= by_1 - dy_1 y_3 - y_4 \\ \dot{y}_3 &= y_1 y_2 - cy_3 \\ \dot{y}_4 &= dy_2 \end{cases} \tag{9}$$

We denote the state of the leader system (9) as $Y = (y_1, y_2, y_3, y_4)$. As the follower system, we take the controlled two-scroll hyperchaotic system

$$\begin{cases} \dot{z}_1 &= a(z_2 - z_1)_p z_2 z_3 - z_4 + v_1 \\ \dot{z}_2 &= bz_1 - dz_1 z_3 - z_4 + v_2 \\ \dot{z}_3 &= z_1 z_2 - cz_3 + v_3 \\ \dot{z}_4 &= dz_2 + v_4 \end{cases} \tag{10}$$

We denote the state of the follower system (10) as $Z = (z_1, z_2, z_3, z_4)$. The synchronization errors are determined as follows:

$$\begin{cases} \varepsilon_1 &= z_1 - y_1 \\ \varepsilon_2 &= z_2 - y_2 \\ \varepsilon_3 &= z_3 - y_3 \\ \varepsilon_4 &= z_3 - y_4 \end{cases} \tag{11}$$

We calculate the dynamics followed by the synchronization error variables.

We obtain the following system for the error dynamics:

$$\begin{cases} \dot{\varepsilon}_1 &= a(\varepsilon_2 - \varepsilon_1) - \varepsilon_4 - p(z_2 z_3 - y_2 y_3) + v_1 \\ \dot{\varepsilon}_2 &= b\varepsilon_1 - \varepsilon_4 - d(z_1 z_3 - y_1 y_3) + v_2 \\ \dot{\varepsilon}_3 &= z_1 z_2 - y_1 y_2 - c\varepsilon_3 + v_3 \\ \dot{\varepsilon}_4 &= d\varepsilon_2 + v_4 \end{cases} \tag{12}$$

In the ISMC design, an integral sliding manifold is defined for each error variable as follows:

$$\begin{cases} \rho_1 &= \varepsilon_1 + \alpha_1 \int_0^t \varepsilon_1(\theta) d\theta \\ \rho_2 &= \varepsilon_2 + \alpha_2 \int_0^t \varepsilon_2(\theta) d\theta \\ \rho_3 &= \varepsilon_3 + \alpha_3 \int_0^t \varepsilon_3(\theta) d\theta \\ \rho_4 &= \varepsilon_4 + \alpha_4 \int_0^t \varepsilon_4(\theta) d\theta \end{cases} \tag{13}$$

From (13), we deduce the following:

$$\begin{cases} \dot{\rho}_1 &= \dot{\varepsilon}_1 + \alpha_1 \varepsilon_1 \\ \dot{\rho}_2 &= \dot{\varepsilon}_2 + \alpha_2 \varepsilon_2 \\ \dot{\rho}_3 &= \dot{\varepsilon}_3 + \alpha_3 \varepsilon_3 \\ \dot{\rho}_4 &= \dot{\varepsilon}_4 + \alpha_4 \varepsilon_4 \end{cases} \tag{14}$$

In the ISMC design, we assume that $\alpha_i > 0$ for $i = 1, 2, 3, 4$.

Based on the exponential reaching law [28], we set the following:

$$\begin{cases} \dot{\rho}_1 &= -\beta_1 sgn(\rho_1) - K_1 \rho_1 \\ \dot{\rho}_2 &= -\beta_2 sgn(\rho_2) - K_2 \rho_2 \\ \dot{\rho}_3 &= -\beta_3 sgn(\rho_3) - K_3 \rho_3 \\ \dot{\rho}_4 &= -\beta_4 sgn(\rho_4) - K_4 \rho_4 \end{cases} \tag{15}$$

By comparing the equations (14) and (15), we get the following:

$$\begin{cases} \dot{\varepsilon}_1 + \alpha_1 \varepsilon_1 &= -\beta_1 sgn(\rho_1) - K_1 \rho_1 \\ \dot{\varepsilon}_2 + \alpha_2 \varepsilon_2 &= -\beta_2 sgn(\rho_2) - K_2 \rho_2 \\ \dot{\varepsilon}_3 + \alpha_3 \varepsilon_3 &= -\beta_3 sgn(\rho_3) - K_3 \rho_3 \\ \dot{\varepsilon}_4 + \alpha_4 \varepsilon_4 &= -\beta_4 sgn(\rho_4) - K_4 \rho_4 \end{cases} \tag{16}$$

We combine the equations (12) and (16) to obtain the following:

$$\begin{cases} a(\varepsilon_2 - \varepsilon_1) - \varepsilon_4 + p(z_2 z_3 - y_2 y_3) + v_1 + \alpha_1 \varepsilon_1 = -\beta_1 sgn(\rho_1) - K_1 \rho_1 \\ b\varepsilon_1 - \varepsilon_4 - d(z_1 z_3 - y_1 y_3) + v_2 + \alpha_2 \varepsilon_2 = -\beta_2 sgn(\rho_2) - K_2 \rho_2 \\ z_1 z_2 - y_1 y_2 - c\varepsilon_3 + v_3 + \alpha_3 \varepsilon_3 = -\beta_3 sgn(\rho_3) - K_3 \rho_3 \\ d\varepsilon_2 + v_4 + \alpha_4 \varepsilon_4 = -\beta_4 sgn(\rho_4) - K_4 \rho_4 \end{cases} \tag{17}$$

From equation (17), we obtain the required sliding mode control law as follows:

$$\begin{cases} v_1 &= -a(\varepsilon_2 - \varepsilon_1) + \varepsilon_4 - p(z_2 z_3 - y_2 y_3) - \alpha_1 \varepsilon_1 - \beta_1 sgn(\rho_1) - K_1 \rho_1 \\ v_2 &= -b\varepsilon_1 + \varepsilon_4 + d(z_1 z_3 - y_1 y_3) - \alpha_2 \varepsilon_2 - \beta_2 sgn(\rho_2) - K_2 \rho_2 \\ v_3 &= -z_1 z_2 + y_1 y_2 + c\varepsilon_3 - \alpha_3 \varepsilon_3 - \beta_3 sgn(\rho_3) - K_3 \rho_3 \\ v_4 &= -d\varepsilon_2 - \alpha_4 \varepsilon_4 - \beta_4 sgn(\rho_4) - K_4 \rho_4 \end{cases} \tag{18}$$

Theorem 1. The new two-scroll hyperchaotic systems (9) and (10) are globally and asymptotically synchronized for all initial conditions $Y(0), Z(0) \in R_4$ by the integral sliding mode controller (18), where the constants $\alpha_i, \beta_i, K_i, (i = 1, 2, 3, 4)$ are all positive.

Proof. We establish this theorem using Lyapunov stability theory [29]. First, we consider the quadratic and positive definite Lyapunov function defined by

$$V(\rho_1, \rho_2, \rho_3, \rho_4) = \frac{1}{2}(\rho_1^2 + \rho_2^2 + \rho_3^2 + \rho_4^2) \tag{19}$$

We determine the time-derivative of V as follows:

$$\dot{V} = \sum_{i=1}^{4} \rho_i \left[-\beta_i sgn(\rho_i) - K_i \rho_i\right] = \sum_{i=1}^{4} \left[-\beta_i |(\rho_i)| - K_i \rho_i^2\right] \tag{20}$$

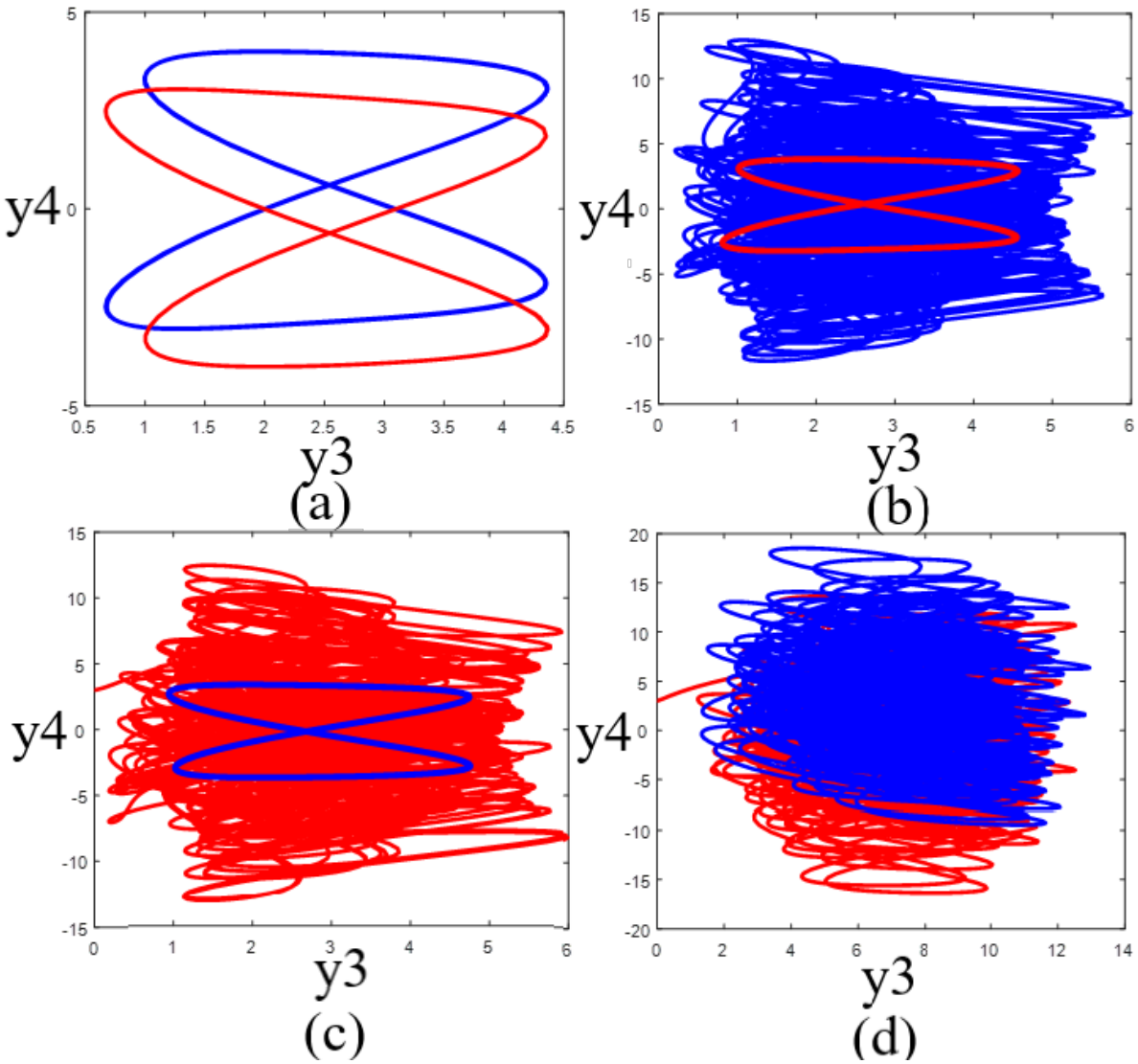

Fig. 18: Matlab plots of different coexisting attractor generated by the new 4-D hyperchaotic system (1) in the (y_3, y_4)-plane.

From (20), we see that $\dot{V}$ is negative definite at all points of R^4. Using Lyapunov stability theory [29], we conclude that $\rho_1(t) \to 0$ as $t \to \infty$ for each $i = 1, 2, 3, 4$.

Hence, it follows that $\varepsilon_i(t) \to 0$ as $t \to \infty$ for each $i = 1, 2, 3, 4$.

This completes the proof. ■

For MATLAB simulations, we take (a, b, c, d, p) =(8,32,3,3,0.2).

We take the sliding constants as $\alpha_i = \beta_i = 0.2$ and $K_i = 20$ for each $i = 1, 2, 3, 4$.

We take the initial state of the new two-scroll hyperchaotic systems (9) and (10)as $Y(0) = (12.3, 4.2, 16.7, 5.4$ and $Z(0) = (5.8, 24.9, 3.1, 14.5)$.

Fig. 19 shows the complete synchronization of the new hyperchaotic systems (9) and (10). Fig. 20 shows the time-history of the synchronization errors.

V. CIRCUIT DESIGN

The implementation of the chaotic circuit based on the new hyperchaotic system is shown in Fig. 21. This circuit was designed with the MultiSIM plathform. The circuit consists of four integrators made using the operational amplifiers U1A, U2A, U3A and U4, each corresponding to the line of the differential equation (1).

By using Kirchhoffs circuit laws, the circuital equations of the designed circuit in Fig. 21 are derivedas follows:

$$\begin{cases} \dot{y}_1 &= \frac{1}{C_1R_1}y_2 - \frac{1}{C_1R_2}y_1 + \frac{1}{10C_1R_3}y_2y_3 - \frac{1}{C_1R_4}y_4 \\ \dot{y}_2 &= \frac{1}{C_2R_5}y_1 - \frac{1}{10C_2R_6}y_1y_3 - \frac{1}{C_2R_7}y_4 \\ \dot{y}_3 &= -\frac{1}{C_3R_8}y_3 + \frac{1}{10C_3R_9}y_1y_2 \\ \dot{y}_4 &= \frac{1}{C_4R_{10}}y_2 \end{cases} \tag{21}$$

Here,y_1, y_2, y_3, y_4 are the voltages across the capacitors C_1, C_2, C_3 and C_4, respectively. We choose the values of the circuital elements as $R_1 = R_2 = 50$ kΩ, $R_3 = 200$ kΩ, $R_4 = R_7 = 400$ kΩ, $R_5 = 12.5$ kΩ, $R_6 = 13.33$ kΩ, $R_8 = R_{10} = 133.33$ kΩ, $R_9 = 40$kΩ, $R_{11} = R_{12} = R_{13} = R_{14} = 100$ kΩ, $C_1 = C_2 = C_3 = C_4 = 1$ nF. The corresponding phase portraits on the oscilloscope are shown in Fig. 21. Multisim simulation have been performed

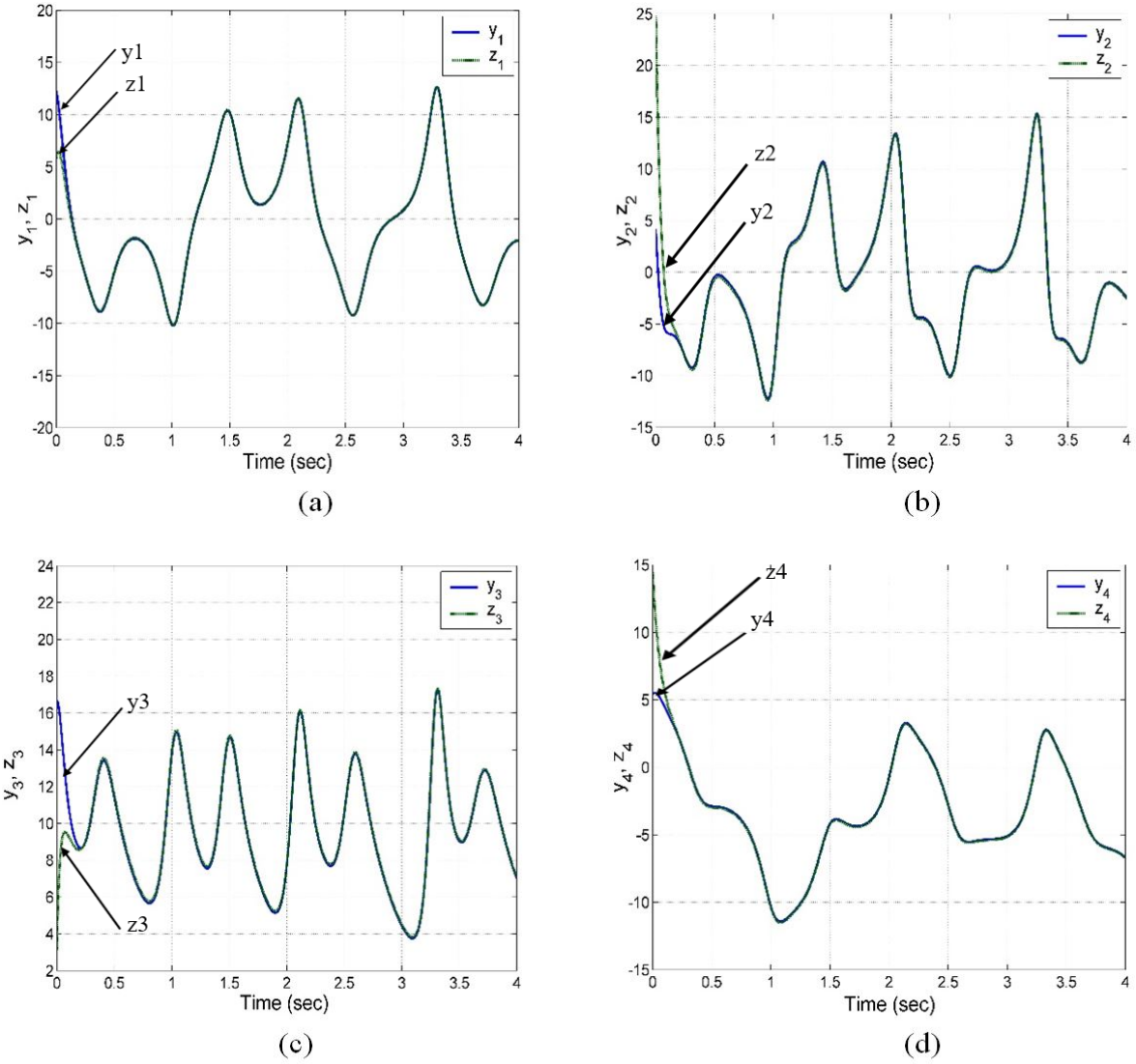

Fig. 19: Complete synchronization of the states of the new systems (9) and (10)

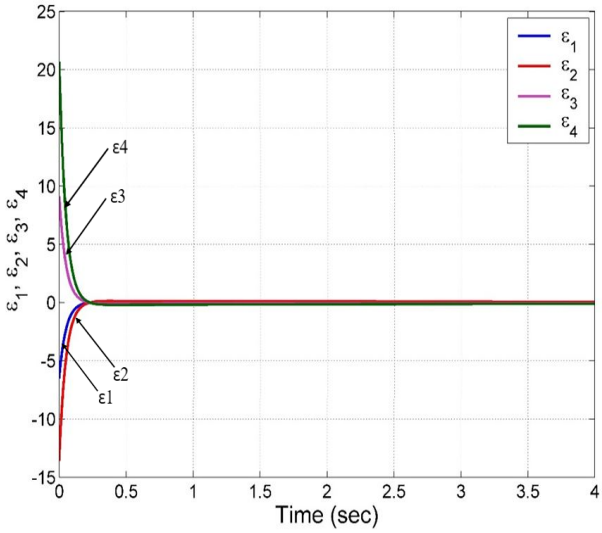

Fig. 20: Time-plot of the synchronization errors between the new systems (9) and (10)

in order to validate the numerical simulation results. A good agreement has been revealed between the results obtained from Multisim software and Matlab software.

VI. CONCLUSION

There is great interest in the modelling and applications of hyperchaotic systems in the chaos literature. A new 4-D two-scroll hyperchaotic system with three quadratic nonlinearities was described in this work. We showed that the new hyperchaotic system is dissipative and it has a unique saddle-point rest point at the origin. Thus, the new hyperchaotic system exhibits a self-excited hyperchaotic attractor. We also proved that the new hyperchaotic system has multistability with coexisting attractors. Next, we made use of integral sliding mode control to achieve global self-synchronization of the new hyperchaotic system taken as leader-follower systems. For real-world applications, we also designed an electronic circuit design of the new two-scroll hyperchaotic system using MultiSim.

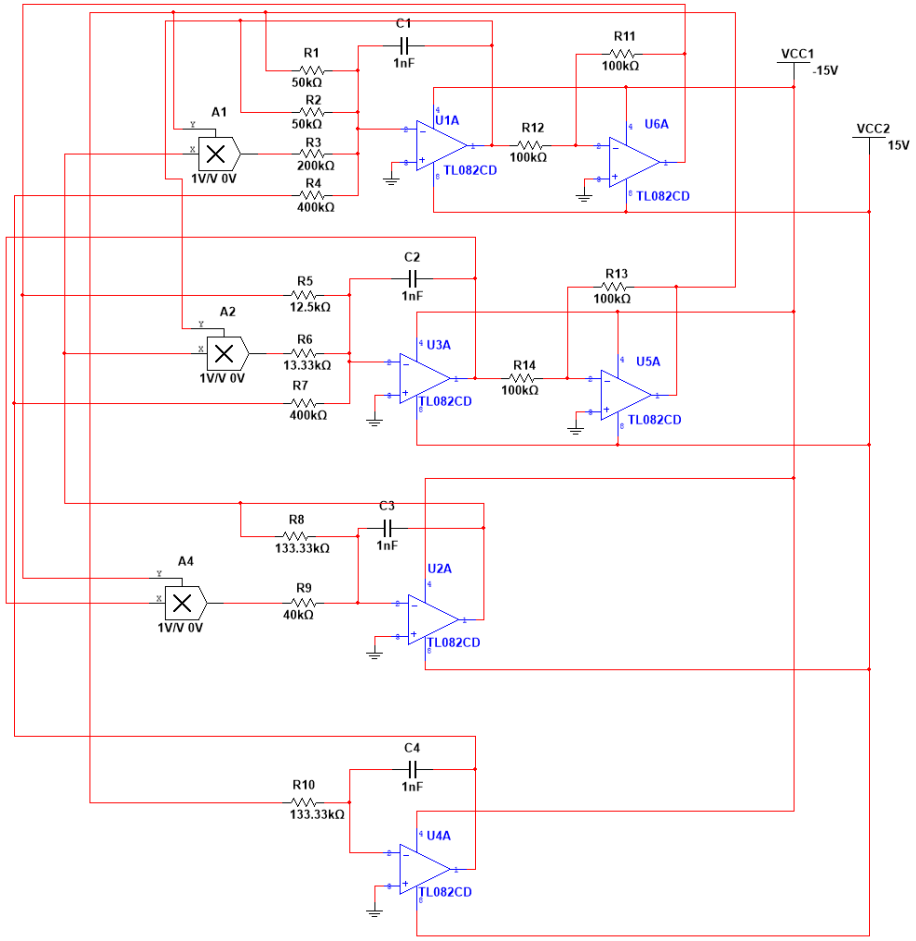

Fig. 21: Circuit Design of the new Hyperchaotic system

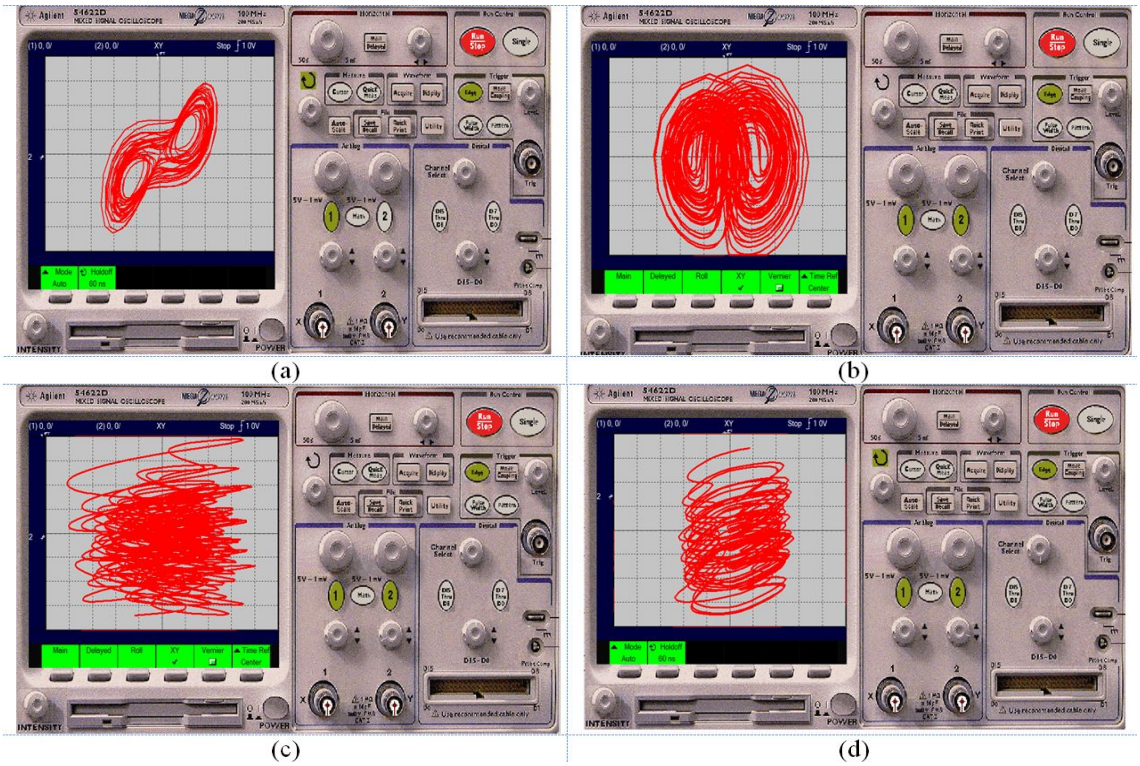

Fig. 22: 2-D oscilloscope outputs of the new Hyperchaotic system (a) $y_1 - y_2$ plane, (b) $y_2 - y_3$ plane,(c) $y_3 - y_4$ plane and (d) $y_1 - y_4$ plane

REFERENCES

[1] Sprott J C, *Elegant chaos: algebraically simple chaotic flows*, Singapore: World Scientific, 2010.

[2] Lin H, Wang C and Tan Y, "Hidden extreme multistability with hyperchaos and transient chaos in a Hopfield neural network affected by electromagnetic radiation." Nonlinear Dynamics, vol. 99, no. 3, pp. 2369-2386, 2020.

[3] Berezowski M, "Chaos predictability in a chemical reactor." International Journal of Bifurcation and Chaos, vol. 30, no. 11, art. id. 2050221, 2020.

[4] De Paula A S and Savi M A, "Comparative analysis of chaos control methods: A mechanical system case study." International Journal of Non-Linear Mechanics, vol. 46, no. 8, pp. 1076-1089, 2011.

[5] Abro, K. A, "Numerical study and chaotic oscillations for aerodynamic model of wind turbine via fractal and fractional differential operators." Numerical Methods for Partial Differential Equations, vol. 38, no. 5, pp. 1180-1194, 2022.

[6] Sambas A, Mohammadzadeh A, Vaidyanathan S, Ayob A F M, Aziz A, Mohamed M A, and Nawi M A A, "Investigation of chaotic behavior and adaptive type-2 fuzzy controller approach for Permanent Magnet Synchronous Generator (PMSG) wind turbine system." AIMS Mathematics, vol. 8, no. 3, pp. 5670-5686, 2023.

[7] Vaidyanathan S, Sambas A, Mamat M and Sanjaya W S M, "A new three-dimensional chaotic system with a hidden attractor, circuit design and application in wireless mobile robot." Archives of Control Sciences, vol. 27, no. 4, pp. 541-554, 2017.

[8] Li C, Sprott J C, Thio W and Zhu H, "A new piecewise linear hyperchaotic circuit."IEEE Transactions on Circuits and Systems II: Express Briefs, vol. 61, no. 12, pp. 977-981, 2014.

[9] Vaidyanathan S, Sambas A, Tlelo-Cuautle E, Abd El-Latif A A, Abd-El-Atty B, Guillén-Fernández O and Ibrahim M A H, "A new 4-D multi-stable hyperchaotic system with no balance point: Bifurcation analysis, circuit simulation, FPGA realization and image cryptosystem."IEEE Access, vol. 9, pp. 62182-62194, 2021.

[10] Kumar K A, Devi R and Rasappan S, "Dynamical Properties of a Modified Chaotic Colpitts Oscillator with Logarithmic Function." Engineering Letters, vol. 30, no. 3, pp. 1107-1119, 2022.

[11] Klioutchnikov I, Sigova M and Beizerov N, "Chaos theory in finance." Procedia computer science, vol. 119, pp. 368-375, 2017.

[12] Sukono, Sambas A, He S, Liu H, Vaidyanathan S, Hidayat Y and Saputra J, "Dynamical analysis and adaptive fuzzy control for the fractional-order financial risk chaotic system." Advances in Difference Equations, vol. 674, no. 1, 1-12, 2020.

[13] Zhang X and Wang C, "Multiscroll hyperchaotic system with hidden attractors and its circuit implementation." International Journal of Bifurcation and Chaos, vol. 29, no. 9, art. id. 1950117, 2019.

[14] Li C, Sprott J C, Kapitaniak T and Lu T, "Multiscroll hyperchaotic system with hidden attractors and its circuit implementation." International Journal of Bifurcation and Chaos, vol. 109, pp. 76-82, 2018.

[15] Tao Y, Cui W, Zhang Z and Shi T, "An Image Encryption Algorithm Based on Hopfield Neural Network and Lorenz HyperChaotic System." IAENG International Journal of Computer Science, vol. 49, no. 4, pp. 1201-1211, 2022.

[16] Li C and Sprott J C, "Multistability in the Lorenz system: a broken butterfly." International Journal of Bifurcation and Chaos, vol. 24, no. 10, art. id. 1450131, 2014.

[17] Li C, Wang X and Chen G, "Diagnosing multistability by offset boosting." Nonlinear Dynamics, vol. 90, no. 2, pp. 1335-1341.

[18] Sambas A, Vaidyanathan S, Zhang S, Putra W T, Mamat M and Mohamed M A, "Multistability in a Novel Chaotic System with Perpendicular Lines of Equilibrium: Analysis, Adaptive Synchronization and Circuit Design." Engineering Letters, vol. 27, no. 4, pp. 744-751, 2019.

[19] Ostrovskii V Y, Rybin V G, Karimov A I, and Butusov D N, "Inducing multistability in discrete chaotic systems using numerical integration with variable symmetry." Chaos, Solitons & Fractals, vol. 165, art. id. 112794, 2022.

[20] Cai G and Tan Z, "Chaos synchronization of a new chaotic system via nonlinear control." Journal of Uncertain systems, vol. 1, no. 3, pp. 235-240, 2007.

[21] Mani P, Rajan R, Shanmugam L and Joo Y H, "Adaptive control for fractional order induced chaotic fuzzy cellular neural networks and its application to image encryption." Information Sciences, vol. 491, pp. 74-89, 2019.

[22] Tian X, Hu X, Gu J, Man C, and Fei S, "Finite-time Control of a Class of Engineering System with Input Saturation via Fractional-order Backstepping Strategy." IAENG International Journal of Computer Science, vol. 50, no. 3, pp. 941-946, 2023.

[23] Takhi H, Kemih K, Moysis L and Volos C, "Passivity based sliding mode control and synchronization of a perturbed uncertain unified chaotic system." Mathematics and Computers in Simulation, vol. 181, pp. 150-169, 2021.

[24] Sambas A, Vaidyanathan S, Zhang X, Koyuncu I, Bonny T, Tuna M, and Kumam P, "A novel 3D chaotic system with line equilibrium: multistability, integral sliding mode control, electronic circuit, FPGA implementation and its image encryption." IEEE Access, vol. 10, pp. 68057-68074, 2022.

[25] Yoon J H, Bak G M and Bae Y, "Fuzzy Control for Chaotic Confliction Model." Journal of Fuzzy Systems, vol. 22, no. 6, pp. 1961-1971, 2020.

[26] Tran X T and Oh H, "Prescribed performance adaptive finite-time control for uncertain horizontal platform systems." Journal of Fuzzy Systems, ISA transactions, vol. 103, 122-130.

[27] A. Wolf, J. B. Swift, H. L. Swinney, and J. A. Vastano, *Physica D*, vol. 16, 1985, pp. 285-317.

[28] S. Vaidyanathan, and C. H. Lien, *Applications of Sliding Mode Control in Science and Engineering*, Berlin: Springer, 2017.

[29] H. K. Khalil, *Nonlinear Systems*, New York: Pearson, 2001.

Mujiarto is a Associate Professor at the Muhammadiyah University of Tasikmalaya, Indonesia since 2014. He received his PhD in Mechanical Engineering from the Unipersitas Pendidikan Indonesia (UPI), Indonesia in 2018. His current research focuses on mechanical engineering, engineering drawing, modelling and advanced Mathematics.

Ahmad Faisal Mohamad Ayob is an Associate Professor in Maritime Technology at the Universiti Malaysia Terengganu. obtained his Ph.D. in Mechanical Engineering from the University of New South Wales @ Australian Defence Force Academy in 2011. His focus area is hull performance design, specifically high-speed boat. Other than hull design, Dr. Faisal is also focusing on software-hardware development, specifically ship simulators with the marine engineering and marine industry. He has published technical manuscripts in journals, conference and chapter in books. Subject taught by Dr. Faisal are Engineering Dynamics and Marine Engineering Design. He served as an Executive Committee member for IEEE-Ocean.

Sundarapandian Vaidyanathan is a Professor at the Research and Development Centre, Vel Tech University, Chennai, India. He earned his D.Sc. in Electrical and Systems Engineering from the Washington University, St. Louis, the USA in 1996. His current research focuses on control systems, chaotic and hyperchaotic systems, backstepping control, sliding mode control, intelligent control, computational science and robotics. He has published three textbooks on mathematics and twelve research books on control engineering. He has published over 410 Scopus-indexed research publications. He has also conducted many workshops on control systems and chaos theory using MATLAB and SCILAB.

Aceng Sambas (Member) is currently a Lecturer at the Muhammadiyah University of Tasikmalaya, Indonesia since 2015. He received his PhD in Mathematics from the Universiti Sultan Zainal Abidin (UniSZA), Malaysia in 2021. His current research focuses on dynamical systems, chaotic signals, electrical engineering, computational science, signal processing, robotics, embedded systems and artificial intelligence. Aceng Sambas is a member of Indonesian Operations Research Association (IORA), and in IAENG is a new member has been received on March 2019.

Khaled Benkouider received the MS degree in Automatic Control from the University of Jijel, Jijel, Algeria, 2015. His MS research was on secure communications based on chaotic systems. He received the Ph.D. degree from the University of Jijel in 2021. He is currently an assistant professor in the department of Electronics at Annaba University, Algeria. His main research interests include chaotic systems, control, delayed systems, LPV systems, transmission security and watermarking

Mohd Kamal Mohd Nawawi is currently an Associate Professor at Universiti Utara Malaysia, Malaysia. He received his Ph.D. in Operations Research from the University of Bradford, England in 2009. Prior to joining as an academician in 2001, he worked as an engineer for more than five years. His current research focuses on computer simulation modeling, industrial engineering, decision support systems, and lean manufacturing. He is a graduate member of the Board of Engineers, Malaysia, and was a member of the Management Science/Operations Research Society of Malaysia (MSORSM), The Malaysian Institute of Statistics (ISMy), and the Malaysian Mathematical Sciences Society (PERSAMA).

Kamal Khalid is currently a Lecturer at Universiti Utara Malaysia (UUM), Malaysia. He joined UUM in 2001 after finishing his B.Sc. and M.Sc. in Statistics from Universiti Kebangsaan Malaysia, Malaysia. His current research interests are mathematical modeling, time series, and forecasting analysis. He is actively supervising and monitoring students' academic projects and industrial training.

Elissa Nadia Madi received BSc. and MSc. in Mathematics from Universiti Malaysia Terengganu (UMT), Malaysia in 2009 and PhD in Computer Science from University of Nottingham, UK in 2018. Her research focuses on the development, adaptation, deployment and evaluation of computational intelligence techniques in inter-disciplinary studies to generate transparent, manageable, informed in decision making method. Current research is towards modelling uncertainty using fuzzy theory based on decision support system. She had authored more than 30 publications in journals and conferences.